

## Membrane Emulsification for the production of uniform poly-N-isopropylacrylamide-coated alginate particles using internal gelation

Mariana Petronela Hanga<sup>1</sup> and Richard G. Holdich<sup>2\*</sup>

<sup>1</sup>Centre for Biological Engineering, Chemical Engineering Department, Loughborough University, Loughborough, Leicestershire, LE11 3TU, UK

<sup>2</sup>Chemical Engineering Department, Loughborough University, Loughborough, Leicestershire, LE11 3TU, UK

\*Corresponding author: Phone: + 44 (0) 1509 222 519

*e-mail address:* [R.G.Holdich@lboro.ac.uk](mailto:R.G.Holdich@lboro.ac.uk)

### ABSTRACT

Alginate particles, crosslinked by calcium ions, have a number of potential biopharmaceutical industry applications due to the biocompatibility of the materials used and formed. One such use is as microcarriers for cell attachment, growth and then detachment without the use of proteolytic enzymes. A straightforward and reproducible method for producing uniform calcium alginate particles with controllable median diameters which employs membrane emulsification and internal gelation (solid particles contained in the dispersed phase) is demonstrated, as well as functionalization of the resulting beads with amine terminated poly N-isopropylacrylamide (pNIPAM) to form temperature responsive particles, by taking advantage of the electrostatic interaction between the carboxyl groups of the alginate and amino groups of the modified pNIPAM. Cell attachment, growth and detachment capabilities of these core-shell structures were assessed and successfully demonstrated by using phase contrast microscopy and fluorescent staining with calcein-AM and ethidium homodimer-1.

The formulation used for the alginate particles avoided non-GRAS chemicals by only using food grade and pharmaceutical grade reagents. The median particle size was controllable within the range between 55  $\mu\text{m}$  to 690  $\mu\text{m}$  and the size distributions produced were very narrow: 'span' values as low as 0.2. When using a membrane pore size of 20  $\mu\text{m}$  no membrane blockage by the suspended calcium carbonate necessary for internal gelation of the alginate particles was observed. Membrane pore openings with diameters of 5 and 10  $\mu\text{m}$  were also tested, but blocked with the 2.3  $\mu\text{m}$  median diameter calcium carbonate solids.

*Keywords:* Stirred Cell; pNIPAM; microbeads; functionalization; microcarriers

## INTRODUCTION

In recent years, there has been an increasing interest in the use of alginate microspheres and microcapsules as encapsulating systems for drugs [1-2] and mammalian cells [3-5] because of the alginate biocompatibility, biodegradability, good mass transfer diffusivity and mechanical properties [6]. Alginate is a polysaccharide obtained from brown algae and it is composed of 1,4-linked- $\beta$ -D-mannuronic acid (M) and  $\alpha$ -L-guluronic acid (G). An important property of alginate is its gelling capabilities in the presence of divalent ions, such as  $\text{Ca}^{2+}$  and stable networks are formed due to the electrostatic interactions between the carboxylic groups in the alginate and  $\text{Ca}^{2+}$ . A commonly used method for producing calcium alginate particles consists of dripping aqueous sodium alginate solution from a syringe into a gelling bath containing calcium chloride, thus forming calcium alginate gel beads by an *external* gelation method [7-8]. The main limitation of this method is the production of gel beads with diameters in the range of millimetres [7-8] which is too large for many applications in the

biomedical field. As a different approach, the *internal* gelation method allows generation of smaller sized alginate particles and this can be applied using emulsification techniques [9-10]. In this method, insoluble calcium carbonate is used as a source of calcium ions when mixed with sodium alginate solution and added to an oil continuous phase thus forming a W/O emulsion. The internal gelation is initiated by increasing the acidity of the emulsion thus calcium ions are released from the insoluble salt, triggering the gelation to form calcium polysaccharide [11]. Emulsification coupled with internal gelation has been frequently reported for the production of alginate gel beads. A common method employs the simple technique of emulsification by stirring [12-13]. However, a critical weakness of this method is that the produced alginate beads vary widely in size and shape and usually have a wide particle size distribution. A different approach, employing single-channel microfluidic devices coupled with internal or external gelation methods [14-15] can produce highly monosized alginate microspheres with coefficients of variation of less than 10%. However, the use of such microfluidic devices is limited by the low flow rates applied generating only very small quantities of particles and with limited scale up possibilities. Another approach, membrane emulsification [16] overcomes some of these limitations by offering the possibility of generating higher quantities of particles, while still maintaining a high control over process parameters, and generating monodispersed emulsions. Several devices coupled with membrane emulsification have been employed for the production of monodispersed microspheres using gas pressure, usually nitrogen, to disperse an aqueous phase into the oil phase [17-19]. However, a major drawback to membrane emulsification is the use of a microfiltration type of membrane for the emulsification when using the internal gelation technique; the finely divided calcium carbonate particles will foul, or block, the membrane when using the sinter type of ceramic or glass membrane [20]. A relatively new approach, compared to the previously reported devices for membrane emulsification, a sieve-type

membrane can be used which has no internal surface or structure on which the particles can deposit. Such a process has been reported previously [18], but in order to achieve the dispersion of solid particulate containing aqueous phase through the sieve-type membrane nanoparticles of calcium carbonate (median size 40 nm) had to be employed, and the membranes used were specialist products from a Chinese nuclear institute with pore sizes between 2.9 and 5.2  $\mu\text{m}$ , providing limited opportunity for scaling to higher productivity. These provided alginate bead sizes between 50 to 150  $\mu\text{m}$ . More recently, a new type of sieve-type membrane has become readily available, with pore size and spacing that may provide conditions appropriate to allow the passage of commercial grades of calcium carbonate in the micrometre size range. It may also be possible to extend the alginate bead size produced to larger sizes, as would be required if using the alginate as a scaffold for microcarriers for mammalian cell culture for example, where sizes of between 100 to 300  $\mu\text{m}$  would be more appropriate. Another application is the encapsulation of cells and the aggregates formed by cells (islet encapsulation), where diameters of alginate particles between 50 and 500  $\mu\text{m}$  are appropriate. Furthermore, no literature currently exists on the use of GRAS components for this application when using membrane emulsification.

The new type of readily available sieve-type membrane is used in a stirred cell device that enables easy control of the drop size [21-24], and hence the resulting size of the formed particles, and it can be used to generate uniform particles. After production of the appropriately sized alginate particles it is possible to functionalise the particle surface, in the case reported here this is by chemisorption of a temperature responsive polymer (amine-terminated pNIPAM) using the electrostatic interactions between the negatively charged carboxylic acid groups in the alginate network and the positively charged amine groups from the modified pNIPAM. The resulting particles will have a temperature responsive surface, which has been shown to have applications in the biomedical field [25-26]. The example

shown here is the attachment of cells to the produced microcarriers, cell growth, followed by cell detachment caused by the thermoresponsive behaviour of the pNIPAM-coated alginate particles. The cell line used for this part of the work was 3T3 cell line (ATCC, USA), which has become the standard fibroblast cell line used as "feeder cells" in human embryonic stem cell research.

### *Dispersed drop size modelling during emulsification*

The equations used in this work were derived in a previous study [27]. Briefly, the model consists of calculating the droplet size from a balance of the capillary force and the drag force acting on a strongly deformed droplet at a single membrane pore:

$$x = \frac{\sqrt{18\tau^2rp^2 + 2\sqrt{81\tau^4rp^4 + 4\tau^2rp^2\gamma^2}}}{3\tau} \quad (1)$$

where  $r_p$  is the pore radius,  $\tau$  is the shear stress,  $\gamma$  is the interfacial tension and  $x$  is the drop diameter.

$$r_{trans} = \frac{D}{2} 1.23(0.57 + 0.35 \frac{D}{T}) (\frac{b}{T})^{0.036} nb^{0.116} \frac{Re}{1000 + 1.43Re} \quad (2)$$

For the Dispersion Cell illustrated in Figure 1, equation (2) can be used to calculate the location of the transitional radius along the paddle-blade radius. The transitional radius is the point at which the rotation changes from a forced vortex to a free vortex where  $b$  is the blade height,  $T$  is the tank width,  $D$  is the stirrer width, and  $nb$  is the number of blades. The Reynolds Number is defined by  $Re = \rho\omega D^2 / 2\pi\eta$ , where  $\rho$  is the continuous phase density,  $\omega$  is the angular velocity and  $\eta$  is the continuous phase coefficient of dynamic viscosity. For the

experimental equipment used in this study,  $H = 16$  cm,  $D = 3.1$  cm,  $nb = 2$ ,  $b = 1.1$  cm and  $T = 3.5$  cm. The boundary layer thickness,  $\delta$ , is defined by the Landau- Lifshitz equation (3) [28].

$$\delta = \sqrt{\frac{\eta}{\rho\omega}} \quad (3)$$

$$\tau = 0.825\eta\omega r \frac{1}{\delta} \quad \text{for } r < r_{\text{trans}} \quad (4)$$

$$\tau = 0.825\eta\omega r_{\text{trans}} \left(\frac{r_{\text{trans}}}{r}\right)^{0.6} \frac{1}{\delta} \quad \text{for } r > r_{\text{trans}} \quad (5)$$

The shear stress in the boundary layer above the membrane surface varies according to equations (4) and (5), for radial positions less than the transitional radius and greater than the transitional radius, respectively. In this work, the maximum shear stress is calculated using equations (4), or (5), with  $r = r_{\text{trans}}$  for a given rotation speed and continuous phase viscosity. The maximum shear stress is then used in equation (1) to provide the predicted drop size, which is then compared to the experimental values obtained in the following work.

## EXPERIMENTAL

### *Materials*

Sodium alginate (food grade) was acquired from Kalys Gastronomie (France). Its viscosity average molecular weight,  $M_v$ , was determined in 0.1M NaCl at 25°C by using an Ostwald capillary viscometer and applying equation (6):

$$[\eta] = 6.9 \times 10^{-4} M_v^{1.13} \quad (6)$$

given by Martinsen et al. [29] for *Laminaria hyperborea* origin sodium alginates, and found to be equal to  $1.59 \times 10^5$  g/mol.

Pharmaceutical grade Miglyol 840 was obtained from Sasol, Germany. According to the manufacturer's description, Miglyol 840 is a propylene glycol diester of saturated plant fatty acids with a viscosity of 10 mPa s. Sorbitan monooleate (Span 80) was supplied by Sigma Aldrich, UK, glacial acetic acid from Fisher Scientific, UK, and amine-terminated poly-N-isopropylacrylamide (pNIPAM) from Sigma Aldrich, UK with an average number molecular weight  $M_n$  of 5500 (used as received). Reverse Osmosis (RO) water was obtained from a Millipore RO system and the acetone used for cleaning purposes was acquired from Sigma Aldrich, UK.

#### *Preparation of W/O emulsions*

Typically, sodium alginate concentrations ranging from 1% wt to 4% wt are employed for the preparation of alginate hydrogels [5, 11, 17]. The dispersed phase was prepared by dissolving sodium alginate using magnetic stirring and heating to 60°C in RO water to achieve a concentration of 1.5% wt. Higher concentrations of sodium alginate (2% wt and 3% wt) were also attempted, but resulted in highly viscous solutions interfering with the membrane emulsification process. Based on these observations, the tests reported here were performed with 1.5% wt sodium alginate solutions. The resultant alginate solution was left to cool down to room temperature after which calcium carbonate, volume median size 2.3  $\mu\text{m}$  and full size distribution shown in Table 1, was added to obtain a solids concentration of 0.5% wt. Before use, the dispersed phase was left to deaerate for at least one hour at room temperature in order to remove any air bubbles that might interfere with the droplet formation. The continuous phase was 1% wt Span 80 in Miglyol 840.

The emulsification process was performed using a Micropore Technologies Ltd (Derbys, UK) Dispersion Cell (Figure 1) equipped with a hydrophobic disc metal membrane. The device presented in Figure 1 is made of a poly(tetrafluoroethylene) (PTFE) base that houses an inlet for the dispersed phase and the metallic disc membrane. On top of the membrane, a glass cylinder is attached by a screwed section and it contains the continuous phase. The Dispersion Cell uses a 24V DC motor to drive a paddle-blade stirrer that provides the shear stress at the membrane's surface necessary for drop detachment. The dispersed phase is injected at the base of the device through the uniform pores of the disc shaped membrane into the continuous phase thus forming an emulsion. The membranes used in this system were also purchased from Micropore Technologies Ltd (Derbys, UK) and were pretreated before use in order to maintain hydrophobicity by soaking in the Miglyol 840.

From an industrial point of view, the Dispersion Cell device is not suitable for use due to its limited membrane area, but it is an excellent tool for studying the effect of process parameters on particle size and size distribution. However, a system based on an oscillating membrane, or pulsed flow, functioning on the same emulsification principles has been reported [21] for higher manufacturing scales. The work presented in this manuscript only focuses on the Dispersion Cell laboratory device presented in Figure 1. Several studies have been performed previously on the Dispersion Cell focusing on its capabilities to produce monodispersed emulsions [22-24]. In this study, this work is extended to the production of highly monodispersed alginate microgel particles using the internal gelation technique (employing dispersed calcium carbonate) forming alginate particles in a size range suitable for biopharmaceutical use. The device uses a 24 V DC motor to drive a paddle-blade stirrer placed above the membrane which provides the shear at the membrane surface. Stirrer speed settings used here ranged from 2 V to 10 V and were expressed as maximum shear stress at the transitional radius calculated using equations (4), or (5), with  $r = r_{\text{trans}}$  for a given rotation



speed and continuous phase viscosity [24]. The main membranes used in this work were disc shaped metal arrays of 20  $\mu\text{m}$  pores with 80  $\mu\text{m}$ , and alternatively 200  $\mu\text{m}$  pore spacing with an effective surface area of 8.54  $\text{cm}^2$ . Additional tests were performed with membranes with pore sizes of 5 and 10  $\mu\text{m}$ , with a pore spacing of 200  $\mu\text{m}$ .

The dispersed phase was injected through the membrane at a constant controlled rate using a syringe pump (KDS Scientific model 101) with injection rates ranging between 0.58 mL/min and 2.2 mL/min. The continuous phase volume used was 100  $\text{cm}^3$  and for each experiment 10  $\text{cm}^3$  of dispersed phase was injected.

The interfacial tension between the Miglyol 840 oil phase, containing surfactant, and the injected alginate aqueous phase was measured using the Du Nouy ring method with an electronic tensiometer (White Electronic Instruments; DB 2KS). The average value of three measurements of the interfacial tension of system was 32 mN/m.

#### *Preparation and characterisation of calcium alginate particles*

Once the W/O emulsion was formed, the resultant emulsion was transferred to a clean, dry beaker and under continuous stirring at 300 rpm, glacial acetic acid was added to dissolve the calcium carbonate and release  $\text{Ca}^{2+}$  to initiate the internal gelation of the alginate droplets, thus forming alginate microgel particles. The gelation was maintained for 30 minutes, after which the particles were washed successively with acetone and then deionized water to remove oil traces. Alginate particle size and size distribution were measured by employing laser light scattering (Malvern Instruments Mastersizer 2000). The uniformity of the size distribution is expressed as the span which is defined as:

$$\text{Span} = \frac{D(0.9) - D(0.1)}{D(0.5)} \quad (7)$$

where D(0.9), D(0.5) and D(0.1) are the particle sizes at which 90%, 50% and 10% of the volume distribution lies on the cumulative curve. Span values of less than 1 are usually reported to be monosized distributions [20]. Photographs of the obtained particles were taken with an optical microscope (Leitz Ergolux). For further analysis some of the beads were dried from acetone at room temperature over a period of several days and their surface investigated by Scanning Electron Microscopy operated at 10 kV (Cambridge Instruments StereoScan 360). Samples were dried and Gold /Palladium sputtered before SEM analysis.

*pNIPAM coating of calcium alginate particles and characterisation of the produced temperature responsive particles*

Amine terminated pNIPAM was dissolved in RO water at room temperature to form solutions of different concentrations: 1, 10, 50, 100, 200, 400, 600 and 800 ppm. The solubility of pNIPAM in cold water at room temperature can be attributed to the ability of the macromolecule to form hydrogen bonds with the water molecules via the amide functional groups. The temperature induced transition of the amine terminated pNIPAM was determined by measuring the absorbance at 560 nm of 5 mg/mL solutions of different pH values with temperature variation between 27°C and 40°C on a microplate reader (BMG Labtech Omega) with a waiting time of 10 minutes between measurements to allow the samples to reach temperature equilibrium. For the coating step, 0.5 g of dried alginate particles were weighed and suspended in 20 mL solutions of different concentrations of amine terminated pNIPAM and then placed on a shaking platform at room temperature for 24 h. It is believed that amino groups from the amine terminated pNIPAM form polyelectrolyte complexes with carboxylic acid groups in the alginate network. The coated beads were retrieved by filtration and used for further analysis. The amounts of polymer adsorbed onto the calcium alginate surface were

determined by measuring the residual polymer concentrations in the solutions after the contact time. A calibration curve was generated by measuring the turbidity values of different polymer concentrations when solutions were kept at a constant temperature of 40°C by using a portable turbidimeter (AF Scientific Inc. Micro TPW). Based on the generated calibration curve the residual concentration of pNIPAM in the contact solution was measured and the amount sorbed on to the particles was calculated by mass balance. A Langmuir type of isotherm was then constructed. In order to confirm the presence of the temperature responsive polymer on the alginate beads, SEM coupled with Energy Dispersive X-ray (EDX) spectroscopy was performed and for visual confirmation, pictures were taken at room temperature (25°C) and at 40°C.

The use of turbidity, calibrated against concentration of concentration of pNIPAM, to determine the mass of pNIPAM sorbed onto the alginate particle surface by mass balance is an unusual one. Superficially, it would be more obvious to use UV/VIS adsorption at a wavelength that is known to adsorb with the pNIPAM molecule, e.g. 270 nm. This was attempted, but this procedure was found to be severely influenced by the presence of sodium alginate which interfered with the analysis. Adsorption wavelengths between 190 and 600 nm were tested, but there was not any wavelength that was found to be free from interference from the sodium alginate present in solution. Hence, the UV/VIS tests were abandoned and the mass of pNIPAM sorbed was determined by turbidity under carefully controlled temperature conditions.

### *3T3 cell tests*

Swiss albino 3T3 cell line (ATCC, USA) was employed for cell tests. The 3T3 mouse fibroblasts were cultured using a high glucose Dulbecco's Modified Eagle's Medium

(DMEM, 4500 mg/L glucose, with L-glutamine and sodium bicarbonate, sterile-filtered, Sigma Aldrich, UK) supplemented with 10% foetal calf serum, heat inactivated (FCS, Sigma Aldrich, UK). Prior to use, the produced core-shell particles were first sterilised by UV exposure for 3 hours, followed by conditioning in complete growth medium for at least one hour at 37°C and 5% CO<sub>2</sub> atmosphere. The generated particles were seeded in Ultra Low Attachment 6-well plates in order to avoid cell attachment on unwanted surfaces, such as culture vessel, in 3 mL of complete growth medium. 3T3 fibroblastic cells were then seeded onto the prepared carriers at a density of 1 x10<sup>5</sup> cells/ well and incubated at 37°C and in a 5% CO<sub>2</sub> atmosphere. Complete medium exchange was performed every two days. All tests were performed in static conditions.

## RESULTS AND DISCUSSION

### *Alginate particle production*

The recipe employed in this work generated spherical shaped micron-sized calcium alginate gel particles as shown in Figure 2. It is well-known that an alginate particle consists of a large volume of water with a low solid content; typically a particle is over 90% water and may only contain 2% solids. Hence the shrinkage and deformation on drying, required for SEM analysis, is substantial. Tests with the 5 and 10 µm pore size membranes showed that membrane blockage occurred quickly, even at the lowest injection rate of 0.58 mL/min. There was no evidence of any blockage when using the 20 µm pore size membrane, with either pore spacing.

In Figure 3 the effect of shear stress generated at the membrane surface on the resulting particle size is illustrated, together with data on the influence of increasing the flow rate of

the injected phase on the particle size and size distribution expressed as span values. It is known that the droplet size is influenced by the injection rate; an increase generates an increase in droplet size [21], and this influence is seen here in Figure 3a. Increasing the rotation speed increases the shear stress on the membrane surface and the droplet formation time shortens, therefore, the size of the produced droplets and thereby particle size decreases. For the system employed here (an array of 20  $\mu\text{m}$  pores and 80  $\mu\text{m}$  pore spacing), a shear stress of 6 Pa (equivalent of 402 rpm) generated alginate particles with sizes between 306  $\mu\text{m}$  and 378  $\mu\text{m}$ , while a shear stress of 42 Pa (equivalent to 1087 rpm) generated particles with sizes in the range of 55  $\mu\text{m}$  and 145  $\mu\text{m}$ . The model presented in Figure 3a is based on the force balance using the maximum shear stress at the transitional radius. The model fit is good at low injection rate (0.58 mL/min), while for higher rates, the produced particles are bigger, but the presented model does not take into consideration the injected phase flow rate. Hence, it should be considered as a model for the minimum particle size produced at the lowest injection rate used.

The size distribution of the generated calcium alginate particles expressed as span values varies between 0.2 and 1.4 as shown in Figure 3(b). In general, a distribution is considered to be monosized if it is smaller than unity [20], but the nearer the value of the span to zero, the more monosized the distribution is.

For comparison, when using a 20  $\mu\text{m}$  pore array with a larger inter-pore spacing (200  $\mu\text{m}$ ), the same pattern is followed, with only marginal differences in particle size and span values. The data is illustrated in Figure 4. These tests were used to determine if an additional force involved in droplet detachment known as ‘push-off’ force was occurring [23]. The ‘push-off’ force involving the ‘push-to-detach’ droplet formation mechanism [30] occurs when most or

all of the membrane's pores become active and droplet formation at one pore is influenced by the presence of other droplets forming at adjacent pores: causing a lower droplet detachment time, and smaller diameter drops of higher uniformity. There is no significant evidence of this effect reported in this work. This was tested over a range of injection rates with similar results to that shown in Figure 4. The reproducibility of the results was assessed by performing triplicate experiments by injecting  $10 \text{ cm}^3$  of dispersed phase at a rate of  $0.58 \text{ mL/min}$  through the  $20 \text{ }\mu\text{m}$  pores of the metal membrane confirming that the method described here is reproducible, as shown in Table 2. Some level of variation was recorded for lower peak shear stress values ( $6 \text{ Pa}$  and  $15 \text{ Pa}$ ), while for  $27 \text{ Pa}$  and  $42 \text{ Pa}$  the results were highly consistent.

The effect of different concentrations of calcium carbonate on the resulting alginate particle size was studied using an array of  $20 \text{ }\mu\text{m}$  pores with  $80 \text{ }\mu\text{m}$  pore spacing at an injection flux of  $0.58 \text{ mL/min}$  and a shear stress of  $27 \text{ Pa}$  as shown in Figure 5. Up to a calcium carbonate concentration of  $5\% \text{ wt}$  there was no evidence of membrane blockage, and a decrease in particle size with calcium carbonate concentration increase was observed, consistent with the formation of a stronger calcium crosslinking within the particles formed, but there were no noticeable advantage in using a higher concentration of calcium carbonate for the further tests. Hence, it was concluded that a  $20 \text{ }\mu\text{m}$  pore size membrane using a concentration of  $0.5\% \text{ wt}$  calcium carbonate suspension was appropriate for the production of alginate particles for functionalization and cell growth.

Alginate forms a good scaffold onto which some form of functionalization can be grafted. One advantage of alginate structures is that they have an appreciable natural internal pore structure, which provides a high surface area for interfacial phenomena to occur [31]. In the

case of cell culture a coupling agent that promotes cell attachment, and promote cell detachment under controllable conditions would be ideal. There has been some considerable interest in using thermoresponsive polymers to achieve this aim [32-34]. Hence, the ability to functionalise the alginate particles formed by membrane emulsification was tested by chemisorption of pNIPAM onto the alginate surface, and cell attachment, growth and detachment were also assessed using the 3T3 cells.

#### *pNIPAM coating of Alginate particles and 3T3 cell tests*

Figure 6(a) shows the calibration curve generated based on turbidity measurements of amine-terminated pNIPAM solutions of different concentrations kept at a constant temperature of 40°C in a circulating water bath. The linear fit of the experimental data is relatively good with an  $R^2$  value of 0.985. Based on this calibration curve, experimental data was collected and fitted to a Langmuir type of isotherm as presented in Figure 6(b) which shows the amount of temperature responsive polymer sorbed on to the surface of the calcium alginate beads with varying pNIPAM concentration in the aqueous phase. The sorption increases with concentration reaching saturation at approximately 4 mg pNIPAM sorbed per gram of alginate bead.

Temperature induced transition of the amine-terminated pNIPAM in aqueous solution was confirmed at different pH values by measuring absorbance at 560 nm. The amine terminated polymer's phase transition temperature is shifted towards a lower temperature value for pH 7, while at pH 5 the temperature response is delayed, as shown in Figure 7. In acidic conditions, the amino groups of the amine-terminated pNIPAM are protonated and it is expected that intra-molecular electrostatic forces develop. As a result, the temperature induced collapse of

the modified polymer chains will occur at a higher temperature which explains the behaviour shown in Figure 7. In order to visually confirm the successful sorption of the temperature responsive polymer onto the alginate scaffold particles, photographs of the particles were taken at room temperature, followed by increasing the temperature to 40°C as shown in Figure 8. A change in colour was observed when increasing the temperature, from transparent and near colourless particles to milky white ones, confirming the phase transition characteristic of the temperature responsive polymer suggesting its presence on the produced alginate particles. To further confirm the successful sorption of the polymer, elemental analysis was performed by SEM coupled with EDX and spectrums were collected from the beads after washing and drying. The elemental analysis is provided in Table 3. The EDX data provides the percentage composition of the elements: carbon, oxygen, nitrogen, calcium and sodium measured at the surface of the particle under investigation. In the case of the alginate beads, i.e. before contact with pNIPAM, there is no nitrogen present as alginate does not contain this element. However, in the case of the pNIPAM coated alginate beads the average weight per cent of nitrogen detected over many tests (at different positions on the surface) is 14%, with a standard deviation of 2.3%. This nitrogen comes from the pNIPAM coating on the alginate beads, which have received repeated washing in water and acetone prior to the EDX tests and demonstrates, therefore, the firm attachment (probably by chemisorption) of the pNIPAM polymer onto the alginate bead surface. The significant level of washing can be demonstrated by reference to the sodium content in the two different beads: it is notable that the alginate particles still demonstrate the presence of sodium, which clearly hasn't been washed out of the beads whereas the pNIPAM coated beads have no measurable sodium present – where the washing must have been more effective.



Finally, the pNIPAM coated beads are shown to be an effective support for the growth of 3T3 fibroblastic cells (ATCC, USA) after sterilisation using UV light, followed by inoculation with the cells and culturing in growth medium supplemented with 10% wt serum. After five days in culture, cell attachment was visualised by phase contrast microscopy, Figure 9(a), and the viability of the cells was checked by staining with Live/Dead staining kit for mammalian cells (Invitrogen, UK) and visualised by fluorescent microscopy as shown in Figure 9(b), where the attachment of the cells on the surface of the beads is apparent. Live healthy cells are stained in green, while dead or damaged cells in red. In Regenerative Medicine one of the recurring challenges is in the ability to attach and grow cells on microcarriers, or beads, followed by the detachment of the cells without the use of enzymatic agents that may damage the cells [35]. In the case of the fibroblasts used here, the detachment was achieved by simply reducing the temperature below the phase transition value, and the cells readily detached from the surface, Figure 9(c). The cells can be seen as small circular entities or clumps of cells that are removed from the bead surface. No enzymatic agent was required for this cell detachment operation.

## CONCLUSIONS

Spherical monodisperse alginate particles with median sizes controllable within the range of 55 to 650  $\mu\text{m}$  and spans of as low as 0.2 were successfully produced by membrane emulsification using a stirred cell system. In that system a simple paddle stirrer provides the shear at the surface of the membrane to detach the drops which are then crosslinked to form particles. It was possible to successfully correlate the drop size formed using the system with a published model for membrane emulsification, relating drop size to shear stress at low dispersed phase injection rates. This correlation can be used to determine the operating

parameters required for scaled-up production of the alginate particles using membrane emulsification employing either pulsed liquid flow, or vibrating membranes. A key feature of the emulsification process used is the membrane pore structure; which is an array of highly uniform pores that pass straight through the membrane with no internal tortuosity. Hence, it is possible to pass suspended solids through the membrane minimising the risk of blockage of the membrane, as would be expected when using microfiltration style membranes for membrane emulsification. This facilitates the possibility of using the internal gelation method in membrane emulsification processes. Inevitably, there has to be a balance between pore size, concentration of solids in the injected phase and the injection rate; as a poor choice can lead to membrane blockage of even the sieve-type of membrane. Tests with membrane pore sizes of 5 and 10  $\mu\text{m}$  were not successful at any injection rate whilst using a calcium carbonate (median size 2.3  $\mu\text{m}$ ) concentration suitable for internal gelation (0.5% wt or more). However, when using a 20  $\mu\text{m}$  pore size membrane no blockage was not noticed at any of the operating conditions of injection rate or dispersed phase concentration. By controlling the stirred speed and the injection rate of the dispersed phase through the membrane pores, it was possible to achieve precise control over particle size and size distribution.

The alginate beads generated by this form of membrane emulsification are in a size range of interest as scaffolds for various biopharmaceutical applications, including microcarriers for cell culture, where some form of functionalising or encapsulating medium can be grafted onto the surface of the alginate. The presence of carboxylic acid groups at the alginate surface can be used to provide chemisorption sites onto which cationic groups can be attached. This was demonstrated by the chemisorption of modified pNIPAM where the amine groups provide the link to the carboxylic acid groups to form a coating of pNIPAM around the alginate particle.

The amounts of polymer adsorbed onto the calcium alginate beads were measured successfully and it was demonstrated to fit a Langmuir type of isotherm. The successful

coating of this thermoresponsive polymer, and the maintenance of its thermoresponsive properties was demonstrated by visual assessment of the particle surface at temperatures above and below the critical transition temperature, as well as EDX analysis of the coated particle surface.

Finally, the beads were demonstrated to be an effective medium for cell growth (after bead sterilisation) and that it was possible to detach the cells that had attached and grown on the bead surface by simply lowering the temperature within the system to below the phase transition temperature (room temperature). This may lead to an effective technique for stem cell growth, and recovery, for Regenerative Medicine applications without the need for enzymatic agents to recover the cells.

## REFERENCES

- [1] Jayant R. D., McShane M. J. and Srivastava R., 2009. Polyelectrolyte-coated alginate microspheres as drug delivery carriers for dexamethasone release. *Drug Delivery*, 16(6), 331–340.
- [2] Ciofani G., Raffa V., Menciassi A., Micera S., Dario P., 2007. A drug delivery system based on alginate microspheres: Mass-transport test and *in vitro* validation. *Biomed Microdevices*, 9, 395–403.
- [3] Smidsrød O., Skjåk-Bræk G., 1990. Alginate as immobilization matrix for cells. *Trends Biotechnol.*, 8, 71–78.

- [4] Workman V.L., Dunnett S.B., Kille P., Palmer D.D., 2007. Microfluidic chip-based synthesis of alginate microspheres for encapsulation of immortalized human cells. *Biomicrofluidics*; 1, 014105-1-9.
- [5] Tan W.H., Takeuchi S., 2007. Monodisperse Alginate Hydrogel Microbeads for Cell Encapsulation. *Adv. Mater.* 19, 2696–2701.
- [6] Webber R.E., Shull K.R., 2004. Strain Dependence of the Viscoelastic Properties of Alginate Hydrogels. *Macromolecules*; 37, 6153-6160.
- [7] Gu F., Amsden B., Neufeld R., 2004. Sustained delivery of vascular endothelial growth factor with alginate beads. *J. of Controlled Release*; 96, 463–472.
- [8] Gombotz W.R., Wee S.F., 1998. Protein release from alginate matrices. *Adv. Drug Delivery Reviews*; 31, 267–285.
- [9] Poncelet D., Lencki R., Beaulieu C. , Halle J. P., Neufeld R. J., Fournier A., 1992. Production of alginate beads by emulsification/internal gelation. I. Methodology. *Appl Microbiol Biotechnol*; 38, 39-45.
- [10] Reis C.P., Neufeld R.J., Vilela S., Ribeiro A.J., Veiga F., 2006. Review and current status of emulsion/dispersion technology using an internal gelation process for the design of alginate particles. *J. of Microencapsulation*; 23(3), 245-257.
- [11] Poncelet, D., 2001, Production of Alginate Beads by Emulsification/Internal Gelation. *Annals of the New York Academy of Sciences*, 944: 74–82.

- [12] Fundueanu G., Esposito E., Mihai D., Carpov A., Desbrieres J., Rinaudo M., Nastruzzi C., 1998. Preparation and characterization of Ca-alginate microspheres by a new emulsification method. *International Journal of Pharmaceutics*; 170, 11–21.
- [13] Zhang F.J., Cheng G.X., Gao Z., Li C.P., 2006. Preparation of Porous Calcium Alginate Membranes/ Microspheres via an Emulsion Templating Method. *Macromol. Mater. Eng.* 291, 485–492.
- [14] Huang K.S., Liu M.K., Wu C.H., Yen Y. T., Lin Y.C., 2007. Calcium alginate microcapsule generation on a microfluidic system fabricated using the optical disk process. *J. Micromech. Microeng.*; 17, 1428–1434.
- [15] Chuah A.M., Kuroiwa T., Kobayashi I., Zhang X., Nakajima M., 2009. Preparation of uniformly sized alginate microspheres using the novel combined methods of microchannel emulsification and external gelation. *Colloids and Surfaces A: Physicochem. Eng. Aspects*; 351, 9–17.
- [16] Peng S. J. and Williams R. A., 1998, Controlled Production of Emulsions using a Cross-flow Membrane: Part I - Droplet Formation from a Single Pore. *Trans IChemE*, 76, Part A: 894 - 901.
- [17] You J.O., Park S.B., Park H.Y., Haam S., Chung C.H., Kim W.S., 2001. Preparation of regular sized Ca-alginate microspheres using membrane emulsification method. *J. microencapsulation*; 18(4), 521-532.

- [18] Liu X.D., Bao D.C., Xue W.M., Xiong Y., Yu W.T., Yu X.J., Ma X.J., Yuan Q., 2003. Preparation of Uniform Calcium Alginate Gel Beads by Membrane Emulsification Coupled with Internal Gelation. *Journal of Applied Polymer Science*, 87, 848–852.
- [19] Zhang Y., Jia X., Wang L., Liu J., Ma G., 2011. Preparation of Ca-Alginate Microparticles and Its Application for Phenylketonuria Oral Therapy. *Ind. Eng. Chem. Res.*; 50, 4106–4112.
- [20] Williams R.A., Peng S.J., Wheeler D.A., Morley N.C., Taylor D., Whalley M., Houldsworth D.W., 1998. Controlled production of emulsions using a crossflow membrane. Part II. Industrial scale manufacture. *Trans. IChemE.*; 76, 902-910.
- [21] Holdich R.G., Dragosavac M.M., Vladisavljevic G.T., Kosvintsev S.R., 2010. Membrane Emulsification with Oscillating and Stationary Membranes. *Ind. Eng. Chem. Res.*; 49, 3810–3817.
- [22] Dragosavac M.M., Sovilj M.N., Kosvintsev S.R., Holdich R.G., Vladisavljevic G.T., 2008. Controlled production of oil-in-water emulsions containing unrefined pumpkin seed oil using stirred cell membrane emulsification. *Journal of Membrane Science*; 322, 178–188.
- [23] Kosvintsev S.R., Gasparini G., Holdich R.G., 2008. Membrane emulsification: Droplet size and uniformity in the absence of surface shear. *Journal of Membrane Science*; 313, 182–189.

[24] Stillwell M.T., Holdich R.G., Kosvintsev S.R., Gasparini G., Cumming I.W., 2007. Stirred Cell Membrane Emulsification and Factors Influencing Dispersion Drop Size and Uniformity. *Ind. Eng. Chem. Res.*; 46, 965-972.

[25] Ward M.A., Georgiou T.K., 2011. Thermoresponsive polymers for biomedical applications. *Polymers*; 3, 1215-1242.

[26] Klouda L., Mikos A.G., 2008. Thermoresponsive hydrogels in biomedical applications. *European Journal of Pharmaceutics and Biopharmaceutics*. 68, 34-45.

[27] Kosvintsev S.R., Gasparini G., Holdich R.G., Cumming I.W., Stillwell M.T., 2005. Liquid-liquid membrane dispersion in a stirred cell with and without controlled shear. *Ind. Eng. Chem. Res.*; 44, 9323.

[28] Landau L.D., Lifshitz E.M., 1959. *Fluid Mechanics*. Pergamon Press: Oxford, U.K.

[29] Martinsen A., Skjåk-Bræk G., Smidsrød O. 1991. Comparison of different methods for determination of molecular weight and molecular weight distribution of alginates. *Carbohydrate Polymers*. 15(2), 171-193.

[30] Zhu J., Barrow D., 2005. Analysis of droplet size during cross-flow membrane emulsification using stationary and vibrating micromachined silicon nitride membranes. *J. Membr. Sci.*; 261, 136.

[31] Thu B., Smidsrød O., Skjak-Braek G. Alginate gels – Some structure-function correlations relevant to their use as immobilization matrix for cells. Wijffels R.H., Buitelaar

R.M., Bucke C., Tramper T. Immobilized cells: Basics and Applications. Progress in Biotechnology, Volume 11. Publisher *Elsevier Science*, The Netherlands, 1996.

[32] Canavan H.E., Cheng X., Graham D.J., Ratner B.D., Castner D.G. Cell sheet detachment affects the extracellular matrix: A surface science study comparing thermal liftoff, enzymatic and mechanical methods. DOI: 10.1002/jbm.a.30297

[33] Halperin A., Kroger M. 2012. Theoretical considerations on mechanisms of harvesting cells cultured on thermoresponsive polymer brushes. *Biomaterials*. 33, 4975-4987.

[34] Wang T., Liu D., Lian C., Zheng S., Liu X. et al. 2011. Rapid cell sheet detachment from alginate semi-interpenetrating nanocomposite hydrogels of PNIPAm and hectorite clay. *Reactive & Functional Polymers*. 71, 447-454

[35] Baumann H. et al. 1979. *Effect of trypsin on the cell surface proteins of hepatoma tissue culture cells*. *J. Biol. Chem.* 254(10), 3935-3946.



## List of Tables

- Table 1 Particle size distribution of the calcium carbonate particles used to provide internal gelation of the alginate
- Table 2 Data from triplicate tests conducted at four shear stresses providing the 10% (D10); 50% (D50) and 90% (D90) drop size values produced and the relative standard deviation between the test values
- Table 3 Alginate particles and pNIPAM-coated particles analysed by SEM coupled with EDX spectra elemental analysis demonstrating a nitrogen peak present only in the latter material

## List of Figures

Figure 1 Schematic illustration of the Dispersion Cell containing a motor driven paddle-blade stirrer placed above the metal membrane: with 20  $\mu\text{m}$  pores and pore spacing of 200  $\mu\text{m}$ , the scale bar represents 100  $\mu\text{m}$

Figure 2 (a) Optical micrographs of uniformly spherical calcium alginate particles generated at an injection rate of 0.58 mL/min and a shear stress of 27 Pa (b) SEM photographs of dried calcium alginate particles

Figure 3 Effect of shear stress at the membrane surface on (a) alginate particle size and (b) uniformity expressed as span values at three dispersed phase injection rates using a membrane of 20  $\mu\text{m}$  pore diameter and 80  $\mu\text{m}$  spacing between pores

Figure 4 Comparison of alginate particles size and size distributions expressed as span values generated at 0.58 mL/min with 20  $\mu\text{m}$  pore size with different spacing between the pores: 80 and 200  $\mu\text{m}$

Figure 5 The effect of calcium carbonate concentration on alginate particle size, other conditions: 20  $\mu\text{m}$  pore array with 80  $\mu\text{m}$  pore spacing at an injection rate of 0.58 mL/min and a shear stress of 27 Pa applied at the membrane surface

Figure 6 a) Calibration curve based on turbidity measurements of amine terminated pNIPAM solutions of different concentrations and b) calculated by mass balance Langmuir type adsorption isotherm of amine terminated pNIPAM onto calcium alginate particles

Figure 7 Effect of pH on the temperature-induced transition of amine-terminated pNIPAM, in a 5 mg/mL aqueous solution; the error bars represent the standard deviation obtained from 4 separate measurements

Figure 8 Photographs of pNIPAM-coated alginate particles below and above the phase transition temperature: at room temperature and 40 degrees Celsius respectively

Figure 9 a) Phase contrast microscopy for visualisation of the attached 3T3 cells on the pNIPAM/alginate particles at Day 5 in culture; b) Fluorescent staining to show viability of the cells after 5 days growth, live healthy cells are stained in green, while dead or damaged cells in red, and c) cells (small circular clumps) shown to detach after lowering temperature below the phase transition value. Scale bars represent 100  $\mu\text{m}$

Table 1 Particle size distribution of the calcium carbonate particles used to provide internal gelation of the alginate

Cumulative amount Undersize (%)	Particle Diameter ( $\mu\text{m}$ )
0	0.17
5	0.60
10	0.88
20	1.40
30	1.72
40	2.03
60	2.69
70	3.09
80	3.56
90	4.28
95	4.90
100	7.70

Table 2 Data from triplicate tests conducted at four shear stresses providing the 10% (D10); 50% (D50) and 90% (D90) drop size values produced and the relative standard deviation between the test values

Shear stress (Pa)	D10		D50		D90	
	Value ( $\mu\text{m}$ )	Relative Standard Deviation (%)	Value ( $\mu\text{m}$ )	Relative Standard Deviation (%)	Value ( $\mu\text{m}$ )	Relative Standard Deviation (%)
6.0	128	5.4	191	5.4	259	5.6
15.0	102	2.6	124	21	156	41
27.0	97	2.2	108	1.5	121	1.9
42.0	98.0	0.4	107	1.9	118	4.2

Table 3 Alginate particles and pNIPAM-coated particles analysed by SEM coupled with EDX spectra elemental analysis demonstrating a nitrogen peak present only in the latter material

Element:	C	O	N	Ca	Na
In alginate beads:					
Average weight%	40	33	0	25	2.0
Standard deviation	5.4	7.0	0	12	0.5
In pNIPAM-coated alginate beads:					
Average weight%	55	27	14	3.4	0
Standard deviation	2.3	1.1	2.3	1.3	0

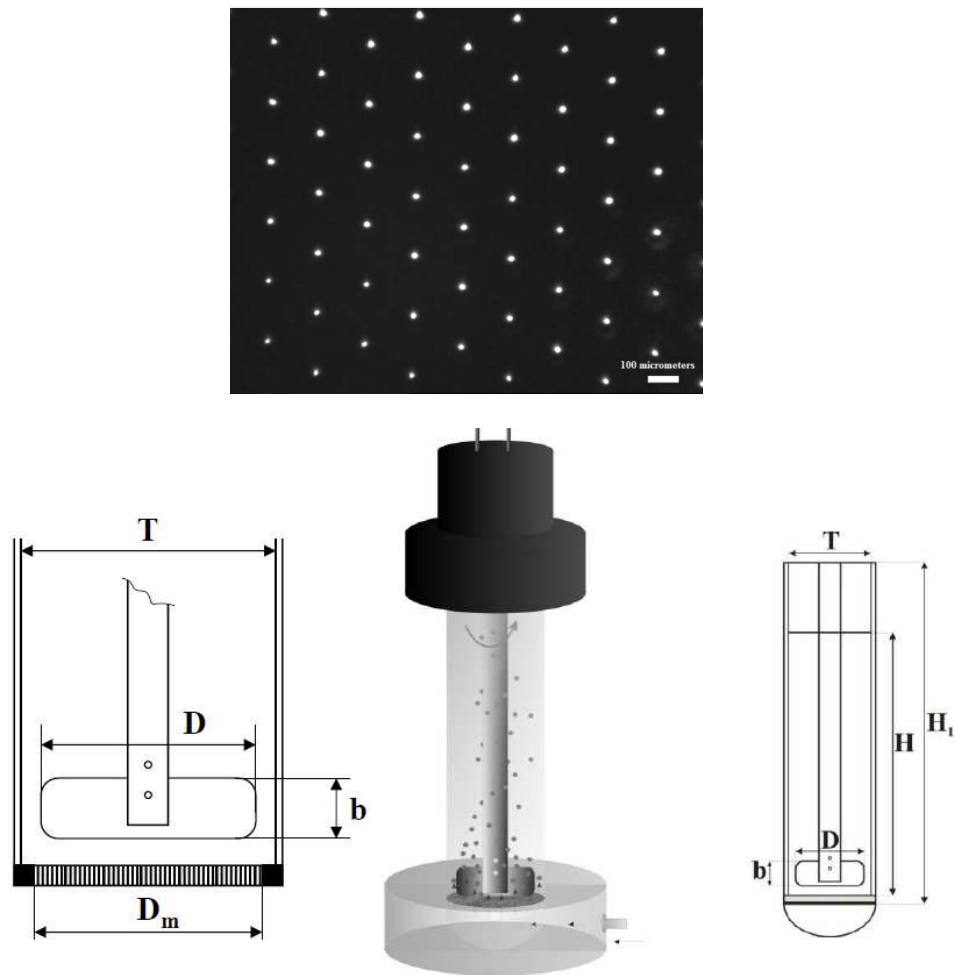


Figure 1 Schematic illustration of the Dispersion Cell containing a motor driven paddle-blade stirrer placed above the metal membrane: with 20  $\mu\text{m}$  pores and pore spacing of 200  $\mu\text{m}$ , the scale bar represents 100  $\mu\text{m}$

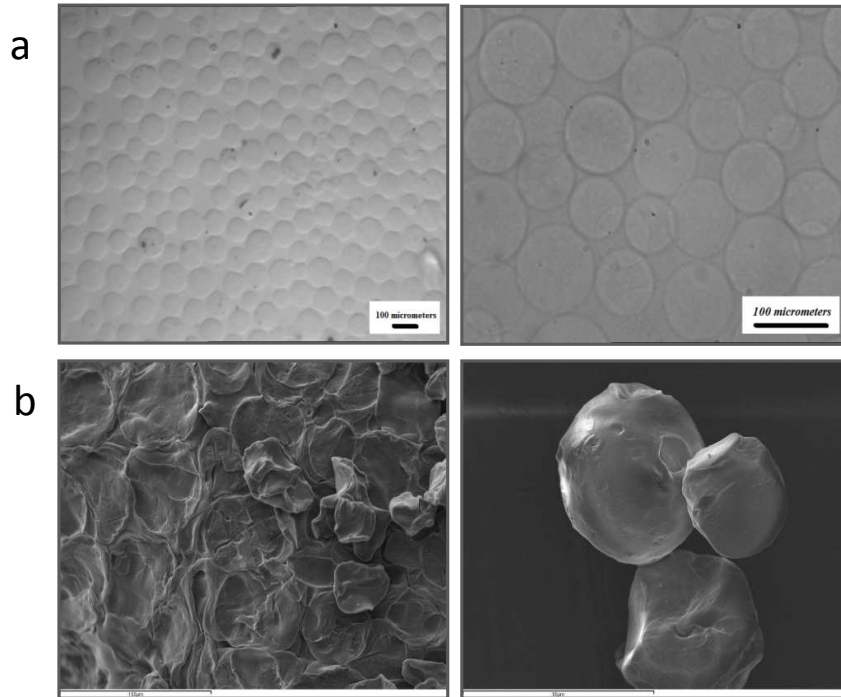
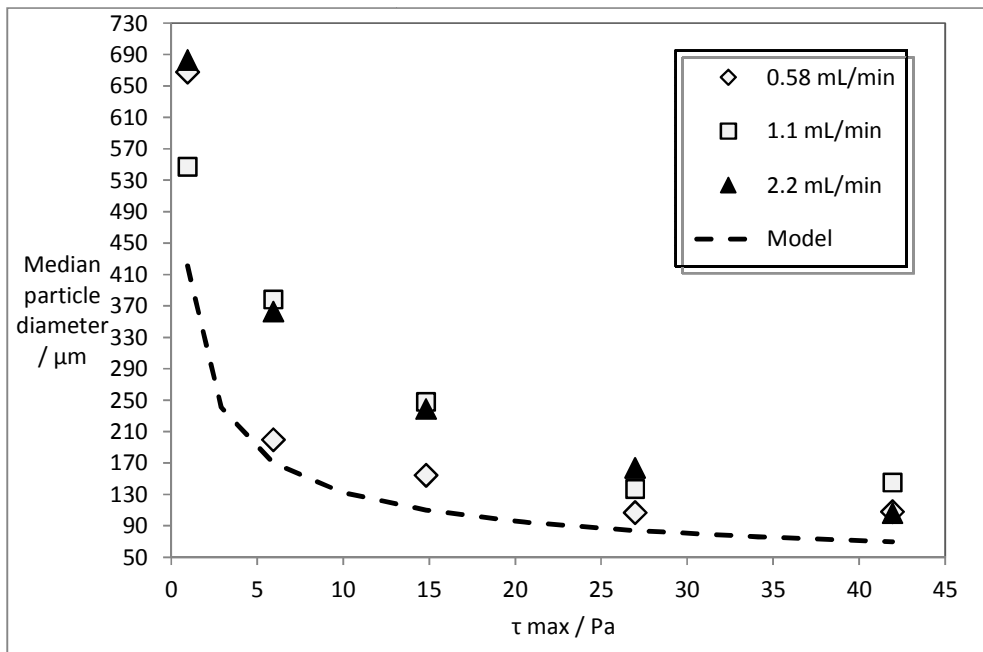


Figure 2 (a) Optical micrographs of uniformly spherical calcium alginate particles generated at an injection rate of 0.58 mL/min and a shear stress of 27 Pa (b) SEM photographs of dried calcium alginate particles



a)



b)

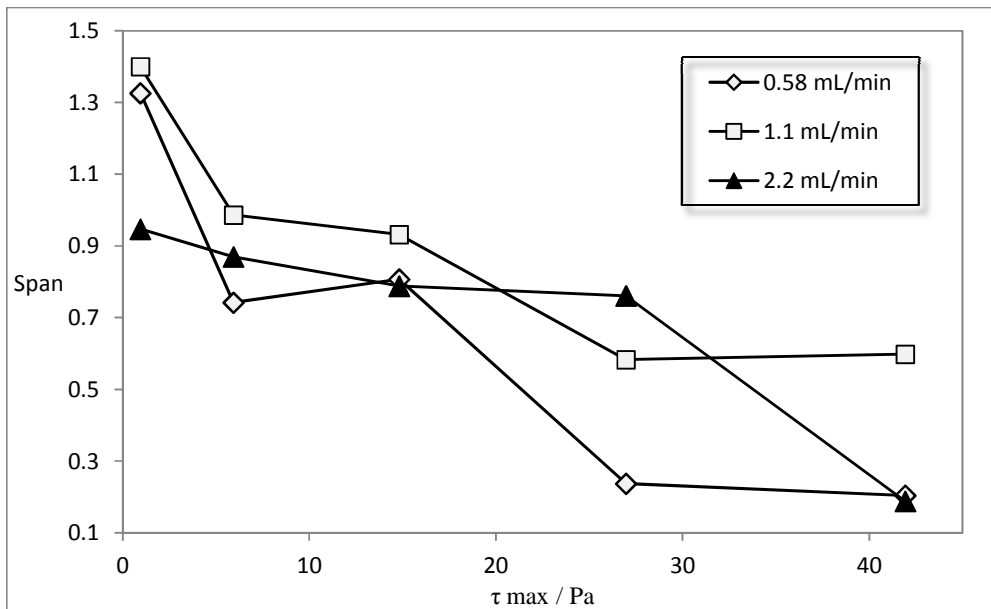


Figure 3 Effect of shear stress at the membrane surface on (a) alginate particle size and (b) uniformity expressed as span values at three dispersed phase injection rates using a membrane of 20  $\mu\text{m}$  pore diameter and 80  $\mu\text{m}$  spacing between pores

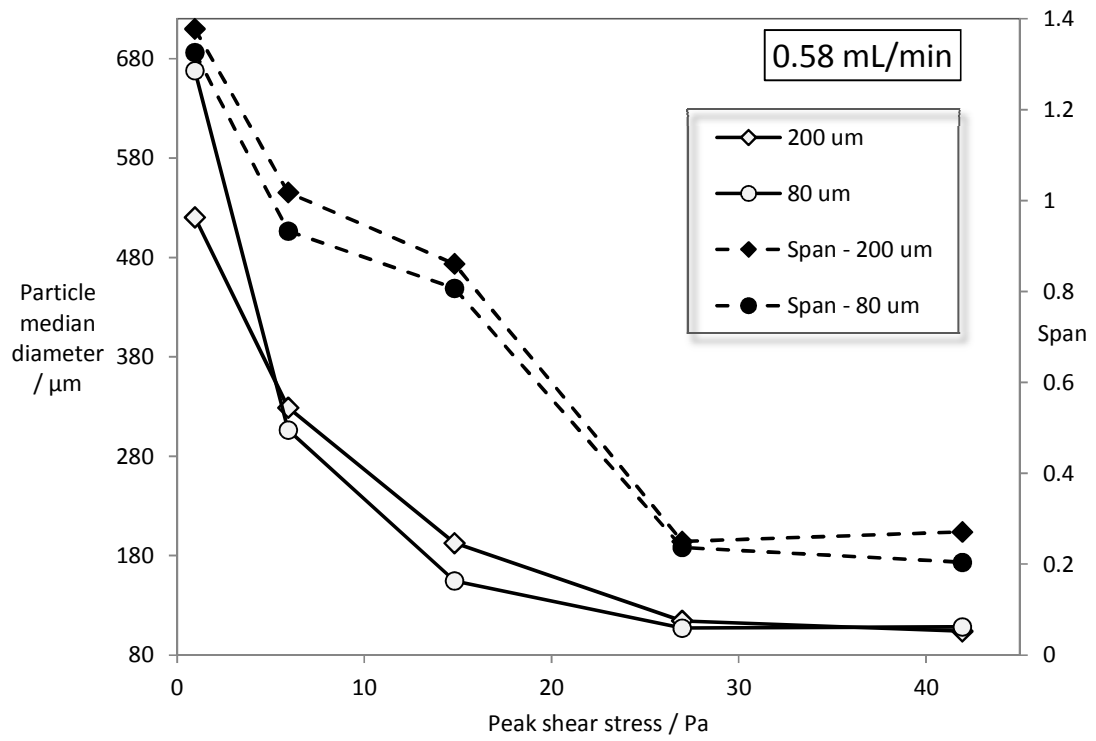


Figure 4 Comparison of alginate particles size and size distributions expressed as span values generated at 0.58 mL/min with 20  $\mu\text{m}$  pore size with different spacing between the pores: 80 and 200  $\mu\text{m}$

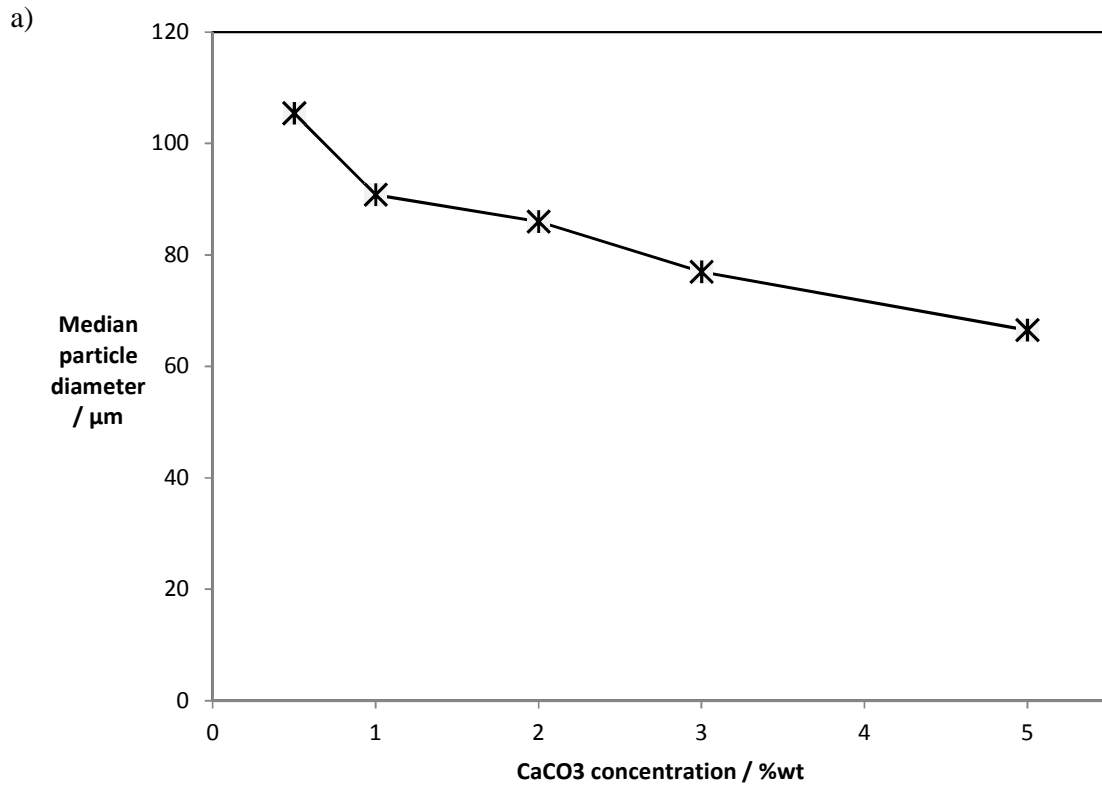


Figure 5 The effect of calcium carbonate concentration on alginate particle size, other conditions: 20  $\mu\text{m}$  pore array with 80  $\mu\text{m}$  pore spacing at an injection rate of 0.58 mL/min and a shear stress of 27 Pa applied at the membrane surface

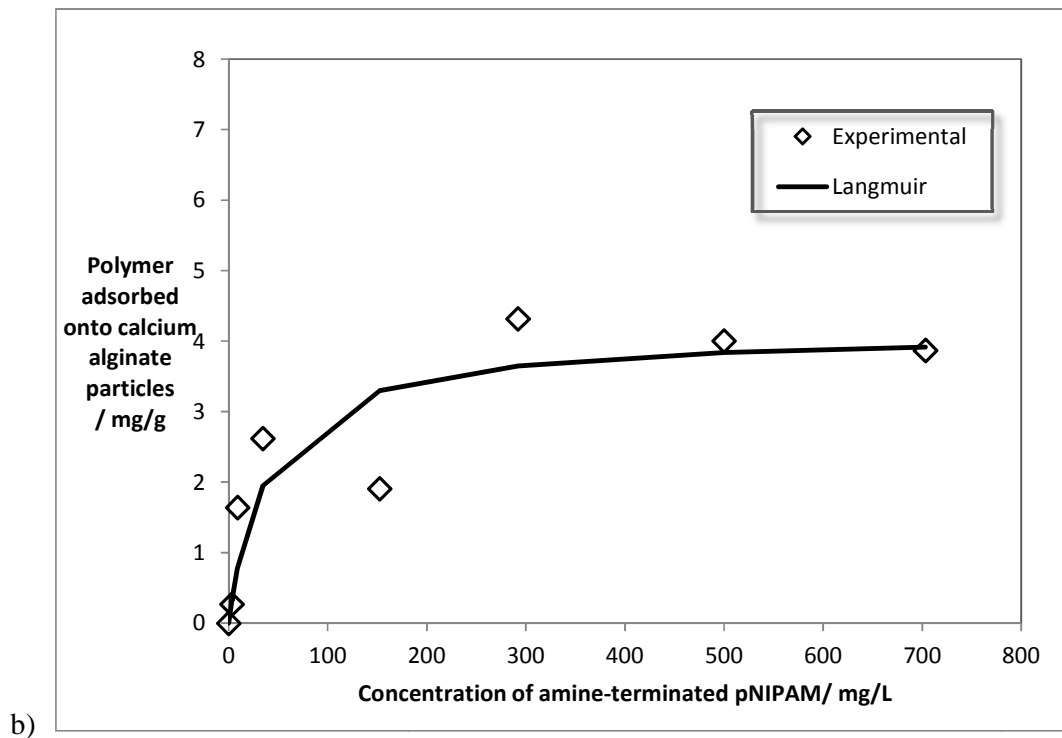
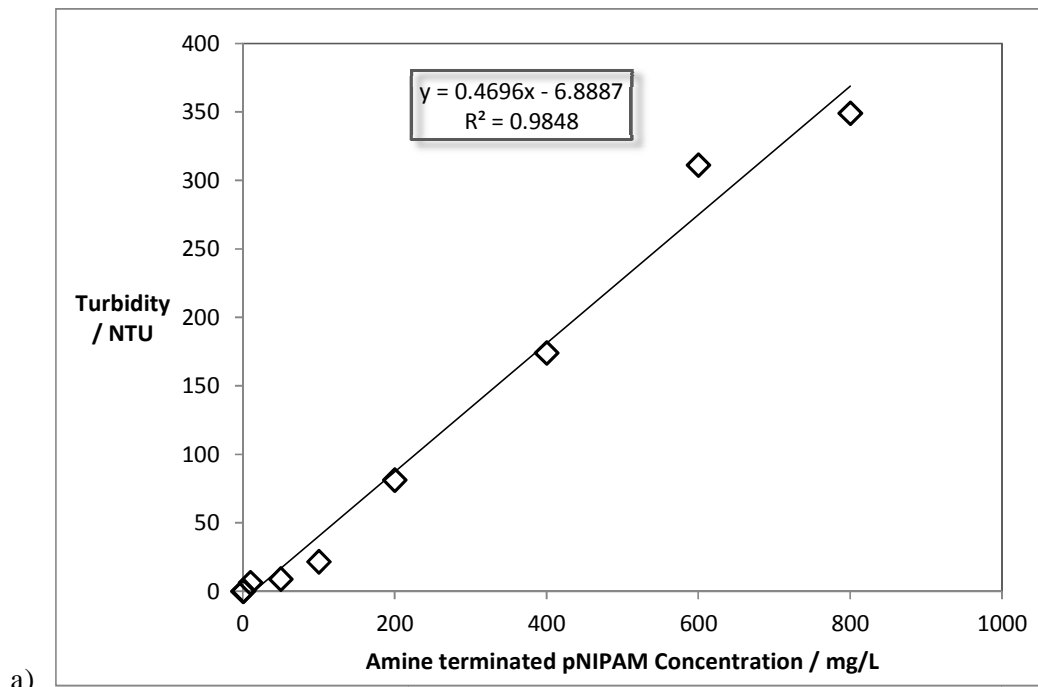


Figure 6 a) Calibration curve based on turbidity measurements of amine terminated pNIPAM solutions of different concentrations and b) calculated by mass balance Langmuir type adsorption isotherm of amine terminated pNIPAM onto calcium alginate particles

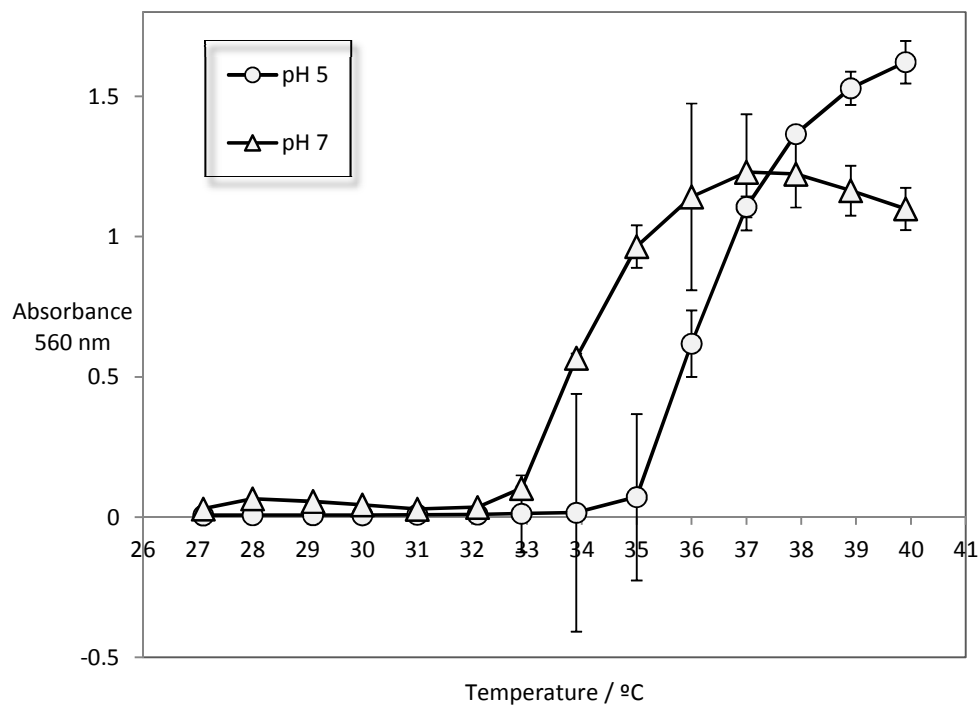


Figure 7 Effect of pH on the temperature-induced transition of amine-terminated pNIPAM, in a 5 mg/mL aqueous solution; the error bars represent the standard deviation obtained from 4 separate measurements

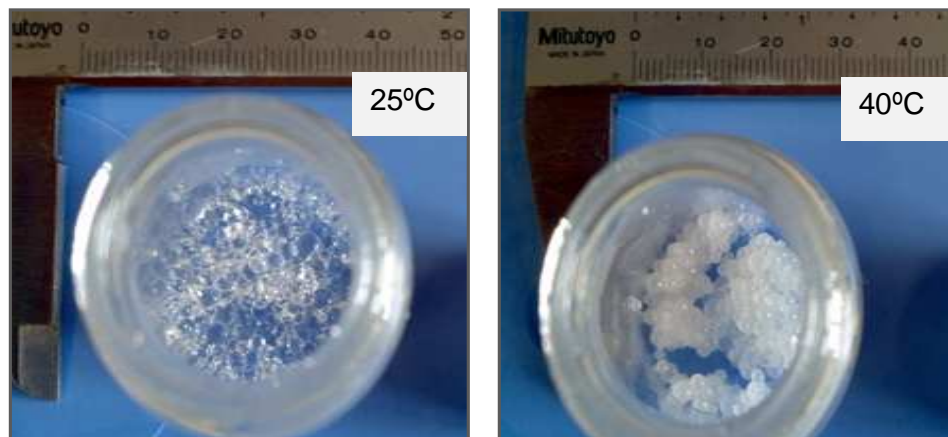
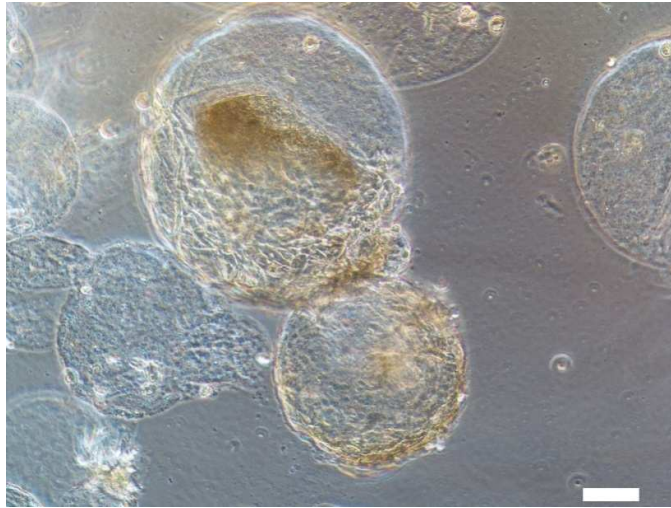


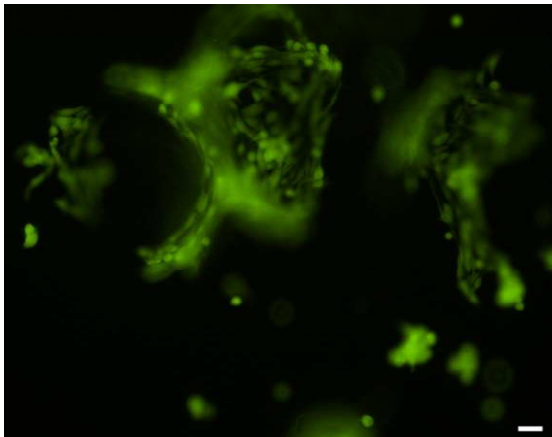
Figure 8 Photographs of pNIPAM-coated alginate particles below and above the phase transition temperature: at room temperature and 40 degrees Celsius respectively

a)

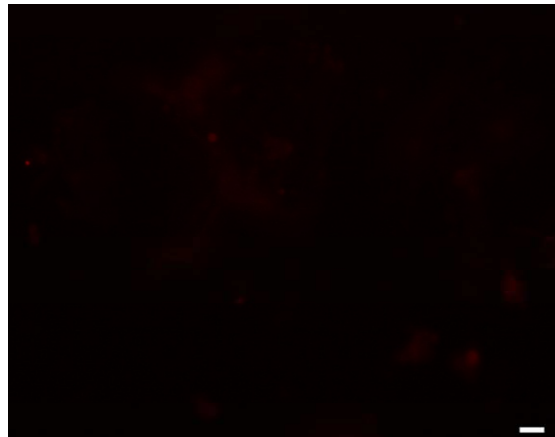


b)

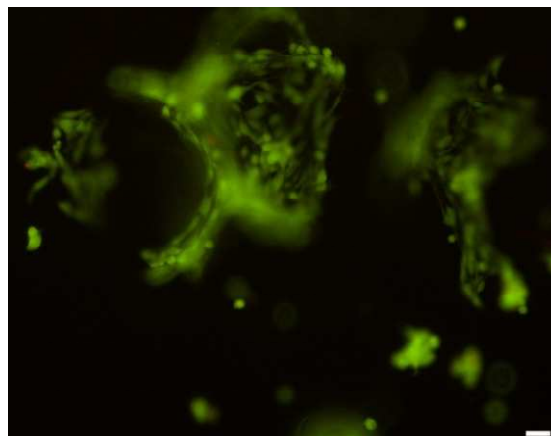
Live



Dead



Merge



c)

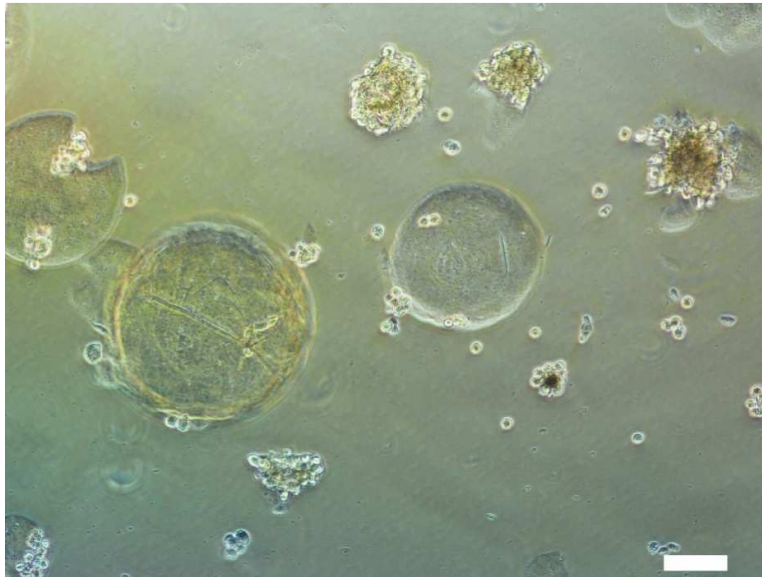


Figure 9 a) Phase contrast microscopy for visualisation of the attached 3T3 cells on the pNIPAM/alginate particles at Day 5 in culture; b) Fluorescent staining to show viability of the cells after 5 days growth, live healthy cells are stained in green, while dead or damaged cells in red, and c) cells (small circular clumps) shown to detach after lowering temperature below the phase transition value. Scale bars represent 100  $\mu\text{m}$